Published in final edited form as:
Mult Scler. 2017 October ; 23(11): 1469–1478. doi:10.1177/1352458516681504.

Translocator positron-emission tomography and magnetic resonance spectroscopy imaging of brain glial cell activation in multiple sclerosis

G. Datta[1], **I.R. Violante**[1], **G. Scott**[1], **G. Zimmerman**[1], **A. Santos-Ribeiro**[1], **E.A. Rabiner**[3,4], **R. N. Gunn**[1,3], **O. Malik**[1], **O. Ciccarelli**[5], **R. Nicholas**[1], and **P.M. Matthews**[1]

[1]Division of Brain Sciences, Imperial College London, UK

[2]Centre for Affective Disorders, Psychological Medicine, Institute of Psychiatry, Psychology and Neuroscience, King's College London, UK

[3]Imanova Ltd, London, UK

[4]Centre for Neuroimaging Sciences, King's College, London, UK

[5]University College London, Institute of Neurology, Queen Square Multiple Sclerosis Centre

Abstract

Background—Multiple sclerosis (MS) is characterized by a diffuse inflammatory response mediated by microglia and astrocytes. Brain translocator protein (TSPO) positron-emission tomography (PET) and [myo-inositol] magnetic resonance spectroscopy (MRS) imaging was used together to assess this.

Objective—To explore the *in vivo* relationships between MRS and PET [^{11}C]PBR28 in MS with a range of brain inflammatory burdens.

Methods—A total of 23 patients were studied. TSPO PET imaging with [^{11}C]PBR28, single voxel MRS and conventional MRI sequences were undertaken. Disability was assessed by Expanded Disability Status Scale (EDSS) and Multiple Sclerosis Functional Composite (MSFC).

Results—[11C]PBR28 uptake and [*myo*-inositol] were not associated. When the whole cohort was stratified by higher [11C]PBR28 inflammatory burden, [*myo*-inositol] was positively correlated to [11C]PBR28 uptake (Spearman's $\rho = 0.685$, $p = 0.014$). Moderate correlations were found between [11C]PBR28 uptake and both MRS creatine normalised *N*-acetyl aspartate (NAA) concentration and grey matter volume. MSFC was correlated with grey matter volume ($\rho = 0.535$, $p = 0.009$). There were no associations between other imaging or clinical measures.

Address for correspondence: Prof. Paul M. Matthews, p.matthews@imperial.ac.uk, E515, Division of Brain Sciences, Department of Medicine, Hammersmith Hospital, DuCane Road, London WC12 0NN, Tel: +0044 207 594 2855.

Declarations
GD is an Imperial Wellcome-GSK Trust Training Fellow in Translational Medicine and Therapeutics and thanks GlaxoSmithKline for personal support in this context. PMM is in receipt of generous personal and research support from the Edmond J Safra Foundation and Lily Safra, the Medical Research Council, the Progressive MS Alliance and the UK Engineering and Physics Science Research Council for aspects of this work. PMM acknowledges consultancy fees (paid to his institution) from Roche, Transparency Life Sciences, IXICO, Adelphi Communications and OrbiMed. He has received honoraria or speakers' fees (also paid to his institution) from Novartis and Biogen and has received research or educational funds from Biogen, Novartis and GlaxoSmithKline.

Europe PMC Funders Author Manuscripts

Conclusions—MRS [*myo*-inositol] and PET [11C]PBR28 measure independent inflammatory processes which may be more commonly found together with more severe inflammatory disease. Microglial activation measured by [11C]PBR28 uptake was associated with loss of neuronal integrity and grey matter atrophy.

Keywords

multiple sclerosis; glia; biomarkers; MRI

Introduction

Multiple sclerosis (MS) is a chronic inflammatory condition characterised by focal and diffuse demyelination and neurodegeneration in the central nervous system (CNS). The brain's chronic inflammatory response includes astrocyte activation and microglial activation, as well as recruitment of peripheral macrophages. This chronic inflammation is associated with neurodegeneration and disability progression.1,2 Conventional magnetic resonance imaging (MRI) detects acute white matter inflammatory lesions and consequent demyelination and gliosis. However, it lacks sensitivity and specificity for quantifying chronic inflammation and the associated neuronal injury.

Magnetic resonance spectroscopy (MRS) enables measurement of a range of brain metabolites in vivo. Two metabolites in relatively high concentration, *myo*-inositol and *N*-acetyl aspartate (NAA), are among those showing pathology-related changes in MS.3 Myoinositol has been proposed as a glial marker, as it is found in high concentrations in activated astrocytes and can be elevated in MS compared with healthy controls.4 Choline, a less specific marker of membrane turnover in glial cells, shows similar changes under some conditions.5 NAA is synthesised in the mitochondria of neurons. Reduced concentrations are associated with neurodegeneration in MS and other diseases.4,6

The relationships between neurodegeneration and activation of the innate immune response could be explored by coupling MRS with positron-emission tomography (PET) using radioligands that bind to the 18 kDa mitochondrial translocator protein (TSPO).7 Activated microglia, macrophages and astrocytes express high levels of TSPO. Several studies using the first-generation TSPO ligand [11C] PK11195 have highlighted extensive multi-focal chronic innate inflammation and its association with disability and future clinical relapses. 1,2,8 More recent work by different groups have further described heterogeneity among lesions within individuals and the inflammatory load in the surrounding white matter.9,10 Newer second-generation TSPO ligands (such as [18F]PBR111 or [11C]PBR28)7 with higher binding affinity for TSPO and less non-displaceable (i.e. non-specific binding) have been developed that may more specifically measure inflammatory changes.11

However, specific interpretation of the increased brain TSPO signal in MS with any of these radioligands is confounded by their potential to reflect activated astrocytes, as well as microglia and macrophages. A limited correlative [11C]PK11195 autoradiographic and histopathological study included in the original report suggested selectivity for activated microglia/macrophages in white matter lesions (WMLs).8 Additional immuno-histopathological reports support this conclusion,12 but the more general relationships

Europe PMC Funders Author Manuscripts

between astrocyte markers and TSPO radioligand binding are poorly defined. Combining TSPO PET and MRS *myo*-inositol offers one approach to assessing their relationship in vivo.

In this study, we sought to explore the in vivo relationships between MRS measures of myo-inositol and PET [11C]PBR28 binding in patients with MS selected to have a wide range of brain inflammatory load and disability. This allowed us to explore also how different measures of neuronal integrity (MRS NAA) and neurodegeneration (normalised grey matter volume) were related to these measures of inflammatory response.

Material and methods

Study population

The study was approved by the West Bromley Research Ethics Committee and the Administration of Radioactive Substances Advisory Committee. Patients had a diagnosis of MS according to the revised McDonald criteria (2010),13 with either relapsing-remitting course or a secondary progressive disease course. None of the participants had been treated with steroids or experienced a clinical relapse within 3 months of their scans. Women who were pregnant or breastfeeding were not eligible to participate. All participants gave written informed consent in accordance with the Declaration of Helsinki. Neurological disability was scored using Expanded Disability Status Scale (EDSS) and the Multiple Sclerosis Functional Composite (MSFC).

TSPO genotyping

TSPO genotype was assessed using a TaqMan-based polymerase chain reaction (Applied Biosystems® QuantStudioTM 7) assay specific for the rs6971 polymorphism in the TSPO gene, as previously described.14 Patients having genotypes associated with low-affinity binding (LAB) were excluded, as they show negligible displaceable binding.14

MRI Scanning

MRI scans were performed on a Siemens 3 Tesla Trio scanner (Siemens Healthcare, Erlangen Germany) equipped with a 32-channel phased-array head coil. Volumetric T1-weighted MPRAGE (Magnetization-Prepared Rapid Acquisition Gradient Echo) images were acquired for all subjects using a 1-mm isotropic resolution sequence, before and 5 minutes after intravenous gadolinium-chelate administration (0.2 mL/kg Gadoteric Acid, Dotarem®; repetition time = 2300 ms, echo time =2.98 ms, inversion time = 9.00 ms with 256 mm × 240 mm × 160 mm field of view). Volumetric T2-weighted FLAIR (fluid-attenuated inversion recovery) three-dimensional (3D) SPACE (Sampling Perfection with Application optimised Contrasts using different flip angle Evolution) images were acquired using a 1-mm isotropic resolution sequence with a 250mm×250mm×160mm field of view (FOV), echo time = 397 ms, repetition time = 5 s, inversion time=1800ms, turbo factor of 141 and 256 × 256 × 160 matrix.

Single voxel MR spectroscopy was acquired in the same session as the other MRI sequences. A sagittal survey image was used to identify the anterior commissure (AC) and

posterior commissure (PC). The spectroscopy voxel was positioned just superior to the lateral ventricles in the midline. The spectroscopy voxel measured 40 mm anteroposterior × 25 mm craniocaudal × 40 mm left–right. The voxel was selected based on recommendations for use of MR spectroscopy in MS patients, with modification of length to accommodate the overall volume in our full population.15

Proton spectra were acquired using a PRESS (Point Resolved Spectroscopy) sequence (repetition time = 2000 ms, echo time = 30 ms, 96 averages, 1024 data points). Magnetic field homogeneity was optimised to a linewidth of ~5Hz over the spectroscopy voxel using the proton signal from water. Water suppression was achieved by a chemically selective saturation, the WET (*w*ater suppression enhanced through *T*1 effects) method.16

MRS analyses

LCModel software (version 6.3) was used for metabolite quantification applying the internal water reference method, accounting for different water content in grey matter, white matter and cerebrospinal fluid.17 LCModel analyses the magnetic resonance spectrum as a linear combination of the basis set of complete model spectra of metabolites from a normal population library.17 Only metabolites with Cramér–Rao bounds <20% were considered. Concentrations of NAA, myo-inositol, glycerophosphocholine and creatine plus phosphocreatine were used in this study. Concentrations in millimole (mM) units were calculated for all metabolites by the software. Patient and MRI system factors (such as radiofrequency receiver properties affected by variability of gain in the amplifiers of the receiver system, head size and position) can influence the resonance intensity in ways the analytical algorithm cannot account for. Our analysis used ‘un-corrected’ concentrations only for the same brain and the same scan session, when normalisation values for metabolite concentrations are identical. Otherwise, we used internal normalisations of metabolite concentration. Creatine and phosphocreatine are present in both neurons and glia. Their summed concentration, referred to as total creatine concentration, shows little or no change in chronic lesions or normal-appearing white matter (NAWM) in MS.18 Total creatine concentration therefore was used as the ‘internal standard’ for normalisation of signals from other metabolites from the same voxel.

PET scanning

PET scanning (Discovery RX PET/CT scanner) was performed with a trans-axial resolution of 5.0 mm and a radial resolution of 5.1mm at 1cm from the centre of the FOV in 3D mode. [11C]PBR28 was injected as an intravenous bolus over approximately 20 seconds at the start of a 90 minutes dynamic PET acquisition. Injected activities for [11C]PBR28 ranged from 223.8 to 379.6 MBq (325.6 ± 34.6 MBq, $n = 44$). Injected mass for different subjects ranged from 1.16 to 8.91 μg (2.75±1.64μg). PET data were reconstructed using filtered back projection, including corrections for attenuation and scatter (based on a low-dose CT acquisition). The dynamic data were binned into 26 frames (durations: 8 × 15 seconds, 3 × 1 minutes, 5 × 2 minutes, 5 × 5 minutes, 5 × 10 minutes).

Radioligand synthesis

Radiosynthesis and quality control were performed on-site, as previously described, obtaining radio-chemical purities of >95%.11

[^{11}C]PBR28 PET Image and Kinetic analysis

T2 FLAIR images were rigidly registered to T1 using FLIRT (FMRIB Software Library v5.0). WMLs were manually segmented on the registered T2 image using Jim software (Xinapse Systems v7). The WML mask was used for lesion-filling the T1 image before segmentation into white matter, grey matter and cerebrospinal fluid using the FSL (FMRIB Software Library v5.0) tools FAST and FIRST.19 Normalised brain volumes were calculated using SIENAX (FMRIB Software Library v5.0).19 A mask of NAWM was created by subtracting the WML mask dilated by 6 mm around its edges in 3D and the resulting mask further eroded by 3mm. The masks of WML, NAWM and grey matter were multiplied by the mask of the spectroscopy voxel to create the respective masks within the spectroscopy voxel.

The T1 image and dynamic PET images were used as inputs for the MIAKAT (Molecular Imaging and Kinetic Analysis Toolbox) software package (www.miakat.org) for kinetic analysis of PET data. For this, PET images were motion corrected using a frame-by-frame realignment algorithm, in which all frames were individually realigned to a reference frame and rigid registered to the MNI (Montreal Neurological Institute) space using SPM5 (Wellcome Trust Centre for Neuroimaging, http://www.fil.ion.ucl.ac.uk/spm). These transformed four-dimensional (4D) PET images were integrated over time to obtain 3D PET summation images in MNI space. The CIC Neuroanatomical Atlas was non-linearly deformed into the individual's space, via mapping of T1-weighted MR imaging data, to obtain a personalised anatomical parcellation of regions of interest, which were used to generate time-activity curves for the caudate and voxel-wise for the whole brain. The whole spectroscopy voxel mask and the WML, NAWM and grey matter masks within the spectroscopy voxel were rigid registered to the MNI space.

The Logan graphical reference method20 using a reference tissue time-activity curve as the input function and model fitting performed with linear regression was used to estimate the distribution volume ratio (DVR) at the voxel level to produce parametric DVR maps, relative to the caudate nucleus volume of distribution (VT). All masks were applied to the PET parametric DVR image to obtain the DVR for the respective regions of interest.

We chose to use a normalised quantitation to allow studies to be conducted without an arterial line. [11C] PBR28 VT has a high test–retest variability of approximately 20%, the major contribution to which appears to come in the blood to tissue transfer modelling.21 Alternatively, reference-based methods show less test–retest variability (5% or less).21 While TSPO is expressed throughout the brain, lower levels of specific binding within a proposed pseudo-reference region do not affect the reliability of the parameter estimates, although this may lead to underestimation of relative binding differences between regions of interest.22 We used the caudate nucleus as a pseudo-reference region as relatively lower

levels of microglial activity and TSPO expression is found in the caudate and normalised standardised uptake ratios are low in caudate compared to other brain regions.12,23

Statistical Analyses

Statistical analyses were performed using SPSS software (IBM, SPSS v22). The Shapiro–Wilk test (with *p*-value <0.05 considered significant) and Q-Q plots for normality found that the following variables did not pass the tests for normality: EDSS (p=0.008), MSFC ($p = 2 \times 10–4$), [11C]PBR28 DVR in NAWM ($p = 0.04$) and in WML ($p = 0.03$) of the spectroscopy voxel.

The non-parametric Spearman's correlation coefficient therefore was used for correlational analyses, unless otherwise stated. Descriptive statistics were reported as median and range, unless otherwise stated. A *p*-value of less than 0.05 was considered significant for all statistical tests. A multivariate linear regression of clinical scores (EDSS or MSFC and its components, 25 foot timed walk, nine hole peg test (9HPT) and three second paced auditory serial addition test (PASAT-3)) was performed using a general linear model with normalised whole brain grey matter volume, TSPO DVR, *myo*-inositol and NAA as predictor variables.

Results

A total of 24 people with clinically definite MS underwent [11C]PBR28 PET, single voxel MRS and structural MRI scanning (Table 1, Figure 1). One patient was excluded from the final analysis because noise artefacts precluded reliable estimates of metabolite concentrations. Of the 23 remaining patients (nine men, median age 48years, range 22–66years) included in the final analysis, 7 had a diagnosis of secondary progressive disease and 16 had relapsing-remitting disease. The median EDSS was 5.0 (range, 1.0–7.0). WMLs were found within the spectroscopy voxel for all patients. None of these lesions was gadolinium enhancing.

Differences in [^{11}C]PBR28 uptake are not explained by brain [*myo*-inositol]

The concentration of *myo*-inositol in the spectroscopy voxel (expressed as either an absolute concentration or as a ratio to total tissue creatine) was not significantly correlated to the TSPO binding measure of [11C]PBR28 DVR within either the whole spectroscopy voxel or the [11C]PBR28 DVR of the NAWM, WML or grey matter within the spectroscopy voxel ($p > 0.05$). The mean PET [11C] PBR28 DVR across the whole spectroscopy voxel was correlated with the DVR of WML within the voxel (Spearman's $\rho = 0.90$, $p < 5 \times 10{-}9$).

We explored *posthoc* whether an association could be found in those people with a higher inflammatory burden. To do this, we divided subjects into two groups based on the median [11C]PBR28 DVR of the whole spectroscopy voxel (1.26). Although there were no correlations between normalised [*myo*-inositol] (concentration of *myo*-inositol as a ratio to total creatine) and the [11C]PBR28 DVR measures for the lower inflammatory subgroup (DVR ⩽ 1.26), for the high inflammatory subgroup (DVR > 1.26) there was a correlation between the normalised [*myo*-inositol] and [11C]PBR28 DVR weighted by WML fraction within the high inflammatory load subgroup (ρ=0.685, $p = 0.014$ (un-corrected), Figure 2(a)). No other correlations were found in the high inflammatory group (DVR > 1.26)

between normalised [*myo*-inositol] and [11C]PBR28 DVR either of the whole spectroscopy voxel or of NAWM or grey matter [11C]PBR28 DVR within the voxel.

We further explored whether there was an association between choline and *myo*-inositol concentrations. There was a moderately significant correlation between *myo*-inositol and choline concentrations ($\rho = 0.547$, $p = 0.007$ ((un-corrected), Figure 2(b)).

Relationships between measures of inflammatory burden and measures of neurodegeneration

We explored the relationships of inflammatory markers ([11C]PBR28 DVR and *myo*-inositol) with measures of neurodegeneration. A moderate correlation was found between the creatine normalised NAA concentration and [11C]PBR28 DVR in WML ($\rho = -0.443$, $p = 0.034$ (un-corrected), Figure 3(a)). The correlation between normalised NAA concentration and the whole voxel [11C]PBR28 DVR was not significant ($\rho=-0.411$, $p=0.051$). We also found a correlation between the whole brain normalised grey matter volume, as a measure of relative neurodegeneration, and [11C]PBR28 DVR weighted by WML fraction in the spectroscopy voxel ($\rho=-0.535$, $p=0.009$, Figure 3(b)). There was no evidence for correlations between *myo*-inositol and either NAA ($\rho=0.238$, $p=0.274$) or the normalised whole brain grey matter volume ($\rho=-0.205$ and $p=0.349$). We did not find significant correlations between either the whole brain normalised grey matter volume and the whole brain [11C]PBR28 DVR ($\rho=-0.236$, $p=0.278$) or the grey matter fraction and the [11C]PBR28 DVR within the voxel ($\rho = 0.07$, $p = 0.75$).

Imaging measures and disability

Disability measured by MSFC was correlated with normalised grey matter volume ($\rho = 0.535$, $p = 0.009$). We found within a general linear model that a large component of disability, as measured by MSFC, was explained by normalised grey matter volume ($F = 19.5$, $p=2\times10-4$). This relationship was driven predominantly by lower and upper limb motor scores (25 foot timed walk, $F=18.8$, $p=0.007$; 9HPT, $F=11.6$, $p=0.003$). We further tested for additional explanatory power from measures here by including the [11C] PBR28 DVR, *myo*-inositol and NAA, but did not find that they added further to the model. We also did not find significant relationships between any of these measures and EDSS.

Discussion

Increased brain TSPO uptake with non-malignant brain pathology could be attributed to either an increased density of activated microglia or to increased astrocytes, as TSPO expression can be elevated in both cell types.7 Histopathological studies in MS have shown that the [*myo*-inositol] detected by MRS signal corresponds to astrocyte activation4 and that increased TSPO expression co-localises with activated microglia.12 We have been able to test the independence of these markers in vivo for the first time in a group of MS patients with a range of inflammatory loads. We did not find a meaningful correlation between MRS [*myo*-inositol] and PET [11C]PBR28 uptake. We propose that changes in the two measures in this population are related to distinct processes or to elements of a common process with different time courses. Similar findings were reported for HIV-positive patients studied using

Europe PMC Funders Author Manuscripts

the first-generation PET radioligand [11C]PK11195 in conjunction with MRS for [*myo*-inositol].24 The results support interpretation of TSPO PET primarily as a marker of activated microglia/macrophages in MS.

Activated astrocytes and microglia are found within and outside lesions at all stages of MS.25 Brex et al.26 highlight the heterogeneity of changes in MRS neurodegenerative and inflammatory markers among lesions and between patients. In our exploratory analyses, we found that under some conditions there may be parallel activation of microglia, reflected in the PET TSPO signal, and astrocyte activation, reflected by MRS [*myo*-inositol]. In this study, in patients with a higher inflammatory load, MRS [*myo*-inositol] and PET [11C]PBR28 uptake in WML were correlated, providing evidence in vivo for the joint activation of astrocytes and microglia under some conditions. Similar observations were made in a study that found the [*myo*-inositol] was associated with higher levels of brain inflammatory pathology in Alzheimer's disease.27

Grey matter volume and MRS NAA are both markers of neurodegeneration.4,6 In this study, we found that higher TSPO uptake within T2 WMLs was correlated with both reduced NAA and grey matter volume. We suggest that this provides evidence that the microglial activation found within T2 WMLs is associated with neurodegeneration, although we cannot infer causation from this cross-sectional study. This is consistent with histopathological findings in MS in which microglial activation is associated with grey matter neurodegeneration.28,29 In vivo clinical studies have shown an association of increased PET [11C] PK11195 uptake in NAWM with greater brain atrophy.2 Both populations of glial cells could contribute to axonal damage.5 However, the lack of a relationship between brain [*myo*-inositol] and measures of neurodegeneration in this study again supports that the TSPO PET and MRS measure are reporting largely independent phenomena or phenomena with different time courses. There is some evidence that astrocyte activation could be antecedent to neurodegeneration with a longer time course.30

We did not find relationships between disability and the inflammatory marker measures, although a well-precedented31 correlation between grey matter atrophy and disability measured with MSFC was observed, despite the limited study power. However, PET TSPO and MRS, as measures of inflammatory state, may be potentially predictive of future change rather than neurodegenerative processes.32,33 This is supported by in vivo PET [11C]PK11195 studies showing correlations between PET TSPO radioligand uptake and measures of disability or likelihood of a diagnosis of clinically definite MS after presentation with the clinically isolated syndrome.33,34 However, a complication of following how baseline brain inflammation relates to future neurodegenerative and disability is that there appear to be different delays between regional brain inflammatory changes and these other processes in patients with MS.25,30,34 Future, longer term longitudinal studies combining MRS and PET TSPO imaging could evaluate their independent predictive value for future neurodegeneration and disability change.

This small study was powered to test for a relatively strong, general relationship between [*myo*-inositol] and PET [11C]PBR28 uptake in MS. While the results distinguish between results from the two measures, a limitation of the study design is that a broad range of

disease was investigated with a relatively small sample size. The possibility of a relationship under some specific conditions cannot be ruled out. If increased TSPO expression and radioligand binding depends on the specific activation phenotypes of astrocytes, the conclusion that PET TSPO radioligand uptake reflects microglial activation predominantly could not be generalised safely. This deserves further histopathological study. However, *post-mortem* studies in MS consistently show that TSPO expression does not appear to be significant in astrocytes.8,12

A fundamental limitation lies in the use of the MRS [*myo*-inositol] as an index of astrogliosis. While there is a strong evidence in support of the approach from correlative neuropathology,4 anabolic and catabolic pathways for *myo*-inositol are expressed in other cell types, as well.5 Additional corroborative observations with other, potential more specific markers of astrocyte activation would support the argument.35

Acknowledgements

The authors thank Dr Maria Davy of GlaxoSmithKline (GSK) for constructive comments on the study design and its early progression and gratefully acknowledge support from the Imperial College Healthcare Trust Biomedical Research Centre.

Funding

The author(s) disclosed receipt of the following financial support for the research, authorship and/or publication of this article: This work was supported, in part, by GSK as part of the Imperial Wellcome-GSK Trust Training Fellowship in Translational Medicine and Therapeutics.

References

1. Giannetti P, Politis M, Su P, et al. Microglia activation in multiple sclerosis black holes predicts outcome in progressive patients: An in vivo [(11)C](R)-PK11195-PET pilot study. Neurobiol Dis. 2014; 65:203–210. [PubMed: 24508617]
2. Versijpt J, Debruyne JC, Van Laere KJ, et al. Microglial imaging with positron emission tomography and atrophy measurements with magnetic resonance imaging in multiple sclerosis: A correlative study. Mult Scler. 2005; 11:127–134. [PubMed: 15794383]
3. Kapeller P, McLean MA, Griffin CM, et al. Preliminary evidence for neuronal damage in cortical grey matter and normal appearing white matter in short duration relapsing-remitting multiple sclerosis: A quantitative MR spectroscopic imaging study. J Neurol. 2001; 248:131–138. [PubMed: 11284131]
4. Bitsch A, Bruhn H, Vougioukas V, et al. Inflammatory CNS demyelination: Histopathologic correlation with in vivo quantitative proton MR spectroscopy. AJNR Am J Neuroradiol. 1999; 20:1619–1627. [PubMed: 10543631]
5. Rae CD. A guide to the metabolic pathways and function of metabolites observed in human brain 1H magnetic resonance spectra. Neurochem Res. 2014; 39:1–36. [PubMed: 24258018]
6. Fu L, Matthews PM, De Stefano N, et al. Imaging axonal damage of normal-appearing white matter in multiple sclerosis. Brain. 1998; 121(Pt 1):103–113. [PubMed: 9549491]
7. Matthews PM, Datta G. Positron-emission tomography molecular imaging of glia and myelin in drug discovery for multiple sclerosis. Expert Opin Drug Discov. 2015; 10:557–570. [PubMed: 25843125]
8. Banati RB, Newcombe J, Gunn RN, et al. The peripheral benzodiazepine binding site in the brain in multiple sclerosis: Quantitative in vivo imaging of microglia as a measure of disease activity. Brain. 2000; 123(Pt 11):2321–2337. [PubMed: 11050032]

9. Colasanti A, Guo Q, Muhlert N, et al. In vivo assessment of brain white matter inflammation in multiple sclerosis with (18)F-PBR111 PET. J Nucl Med. 2014; 55:1112–1118. [PubMed: 24904112]
10. Rissanen E, Tuisku J, Rokka J, et al. In vivo detection of diffuse inflammation in secondary progressive multiple sclerosis using PET imaging and the radioligand 11C-PK11195. J Nucl Med. 2014; 55:939–944. [PubMed: 24711650]
11. Guo Q, Owen DR, Rabiner EA, et al. Identifying improved TSPO PET imaging probes through biomathematics: The impact of multiple TSPO binding sites in vivo. Neuroimage. 2012; 60:902–910. [PubMed: 22251896]
12. Cosenza-Nashat M, Zhao ML, Suh HS, et al. Expression of the translocator protein of 18 kDa by microglia, macrophages and astrocytes based on immunohistochemical localization in abnormal human brain. Neuropathol Appl Neurobiol. 2009; 35:306–328. [PubMed: 19077109]
13. Polman CH, Reingold SC, Banwell B, et al. Diagnostic criteria for multiple sclerosis: 2010 revisions to the McDonald criteria. Ann Neurol. 2011; 69:292–302. [PubMed: 21387374]
14. Owen DR, Yeo AJ, Gunn RN, et al. An 18-kDa translocator protein (TSPO) polymorphism explains differences in binding affinity of the PET radioligand PBR28. J Cereb Blood Flow Metab. 2012; 32:1–5. [PubMed: 22008728]
15. Bagory M, Durand-Dubief F, Ibarrola D, et al. Implementation of an absolute brain 1H-MRS quantification method to assess different tissue alterations in multiple sclerosis. IEEE Trans Biomed Eng. 2012; 59:2687–2694. [PubMed: 21768043]
16. Ogg RJ, Kingsley PB, Taylor JS, et al. WET, a T1- and B1-insensitive water-suppression method for in vivo localized 1H NMR spectroscopy. J Magn Reson B. 1994; 104:1–10. [PubMed: 8025810]
17. Provencher SW. Estimation of metabolite concentrations from localized in vivo proton NMR spectra. Magn Reson Med. 1993; 30:672–679. [PubMed: 8139448]
18. Sarchielli P, Presciutti O, Pelliccioli GP, et al. Absolute quantification of brain metabolites by proton magnetic resonance spectroscopy in normal-appearing white matter of multiple sclerosis patients. Brain. 1999; 122(Pt 3):513–521. [PubMed: 10094259]
19. Smith SM, Zhang Y, Jenkinson M, et al. Accurate, robust, and automated longitudinal and cross-sectional brain change analysis. Neuroimage. 2002; 17:479–489. [PubMed: 12482100]
20. Logan J, Fowler JS, Volkow ND, et al. Distribution volume ratios without blood sampling from graphical analysis of PET data. J Cereb Blood Flow Metab. 1996; 16:834–840. [PubMed: 8784228]
21. Collste K, Forsberg A, Varrone A, et al. Test-retest reproducibility of [(11)C]PBR28 binding to TSPO in healthy control subjects. Eur J Nucl Med Mol Imaging. 2016; 43:173–183. [PubMed: 26293827]
22. Salinas CA, Searle GE, Gunn RN. The simplified reference tissue model: Model assumption violations and their impact on binding potential. J Cereb Blood Flow Metab. 2015; 35:304–311. [PubMed: 25425078]
23. Guo Q, Owen DR, Rabiner EA, et al. A graphical method to compare the in vivo binding potential of PET radioligands in the absence of a reference region: Application to [11C]PBR28 and [18F]PBR111 for TSPO imaging. J Cereb Blood Flow Metab. 2014; 34:1162–1168. [PubMed: 24736889]
24. Garvey LJ, Pavese N, Ramlackhansingh A, et al. Acute HCV/HIV coinfection is associated with cognitive dysfunction and cerebral metabolite disturbance, but not increased microglial cell activation. PLoS ONE. 2012; 7:e38980. [PubMed: 22808022]
25. Popescu BF, Pirko I, Lucchinetti CF. Pathology of multiple sclerosis: Where do we stand? Continuum. 2013; 19:901–921. [PubMed: 23917093]
26. Brex PA, Parker GJ, Leary SM, et al. Lesion heterogeneity in multiple sclerosis: A study of the relations between appearances on T1 weighted images, T1 relaxation times, and metabolite concentrations. J Neurol Neurosurg Psychiatry. 2000; 68:627–632. [PubMed: 10766895]
27. Murray ME, Przybelski SA, Lesnick TG, et al. Early Alzheimer's disease neuropathology detected by proton MR spectroscopy. J Neurosci. 2014; 34:16247–16255. [PubMed: 25471565]

28. Magliozzi R, Howell OW, Reeves C, et al. A gradient of neuronal loss and meningeal inflammation in multiple sclerosis. Ann Neurol. 2010; 68:477–493. [PubMed: 20976767]
29. Vercellino M, Masera S, Lorenzatti M, et al. Demyelination, inflammation, and neurodegeneration in multiple sclerosis deep gray matter. J Neuropathol Exp Neurol. 2009; 68:489–502. [PubMed: 19525897]
30. Llufriu S, Kornak J, Ratiney H, et al. Magnetic resonance spectroscopy markers of disease progression in multiple sclerosis. JAMA Neurol. 2014; 71:840–847. [PubMed: 24839987]
31. De Stefano N, Filippi M, Miller D, et al. Guidelines for using proton MR spectroscopy in multicenter clinical MS studies. Neurology. 2007; 69:1942–1952. [PubMed: 17998486]
32. Audoin B, Ibarrola D, Malikova I, et al. Onset and underpinnings of white matter atrophy at the very early stage of multiple sclerosis – A two-year longitudinal MRI/MRSI study of corpus callosum. Mult Scler. 2007; 13:41–51. [PubMed: 17294610]
33. Giannetti P, Politis M, Su P, et al. Increased PK11195-PET binding in normal-appearing white matter in clinically isolated syndrome. Brain. 2015; 138:110–119. [PubMed: 25416179]
34. Politis M, Giannetti P, Su P, et al. Increased PK11195 PET binding in the cortex of patients with MS correlates with disability. Neurology. 2012; 79:523–530. [PubMed: 22764258]
35. Parker CA, Nabulsi N, Holden D, et al. Evaluation of 11C-BU99008, a PET ligand for the imidazoline2 binding sites in rhesus brain. J Nucl Med. 2014; 55:838–844. [PubMed: 24711648]

Europe PMC Funders Author Manuscripts

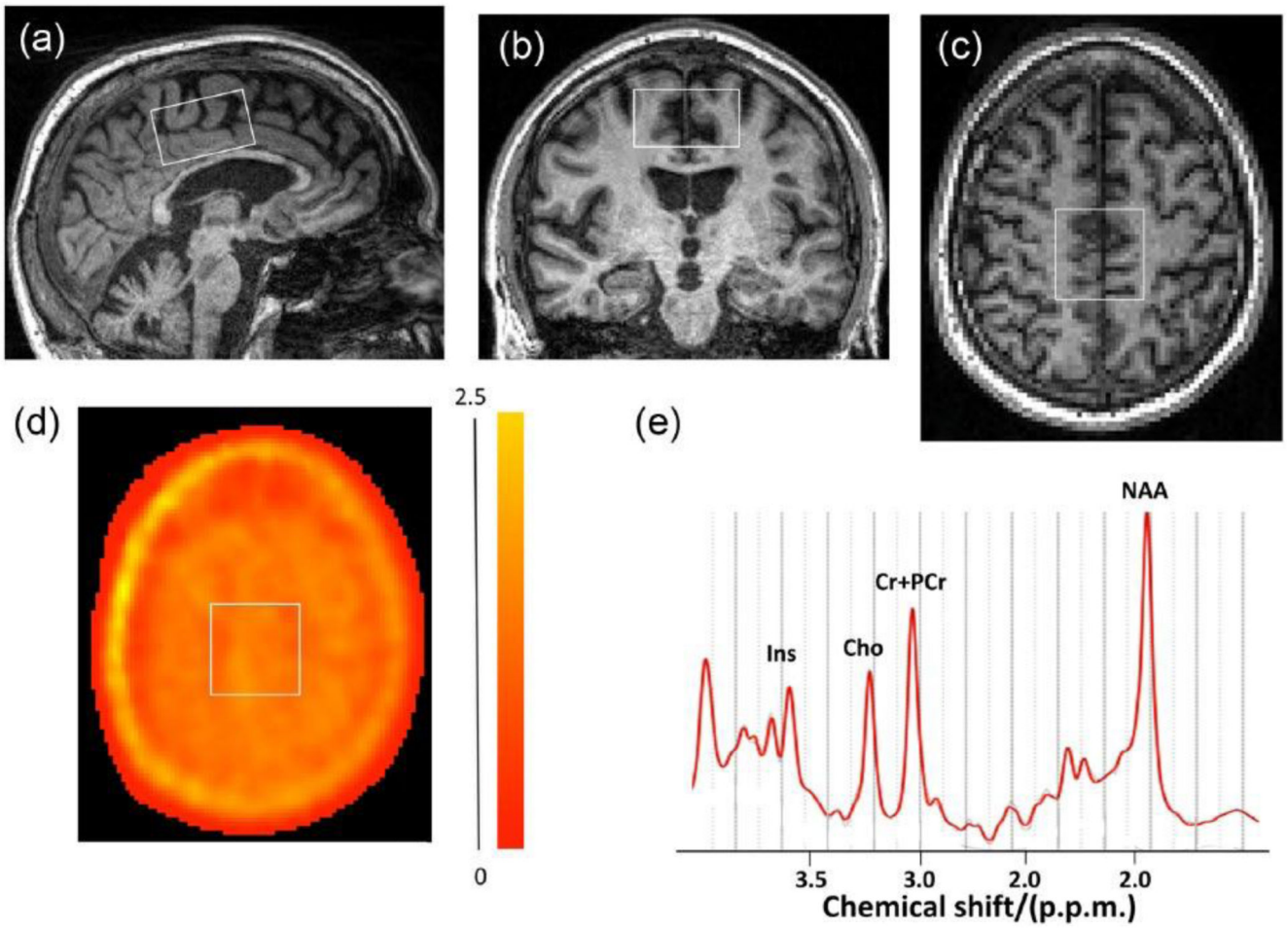

Figure 1.

Placement of spectroscopy voxel shown in (a) sagittal, (b) coronal and (c) axial image planes. (d) A parametric PET [11C]PBR28 distribution volume ratio (DVR) image overlaid with an outline of the placement spectroscopy voxel in the axial MRI plan corresponding to (c) is shown. The colour bar to the right of (d) provides a key to the voxel-wise DVR values in the parametric PET image. (e) A representative MR spectrum for a patient.

Ins: myo-inositol; Cho: choline; Cr+PCr: creatinine and phosphocreatinine; NAA: *N*-acetyl aspartate; p.p.m.: parts per million.

Europe PMC Funders Author Manuscripts

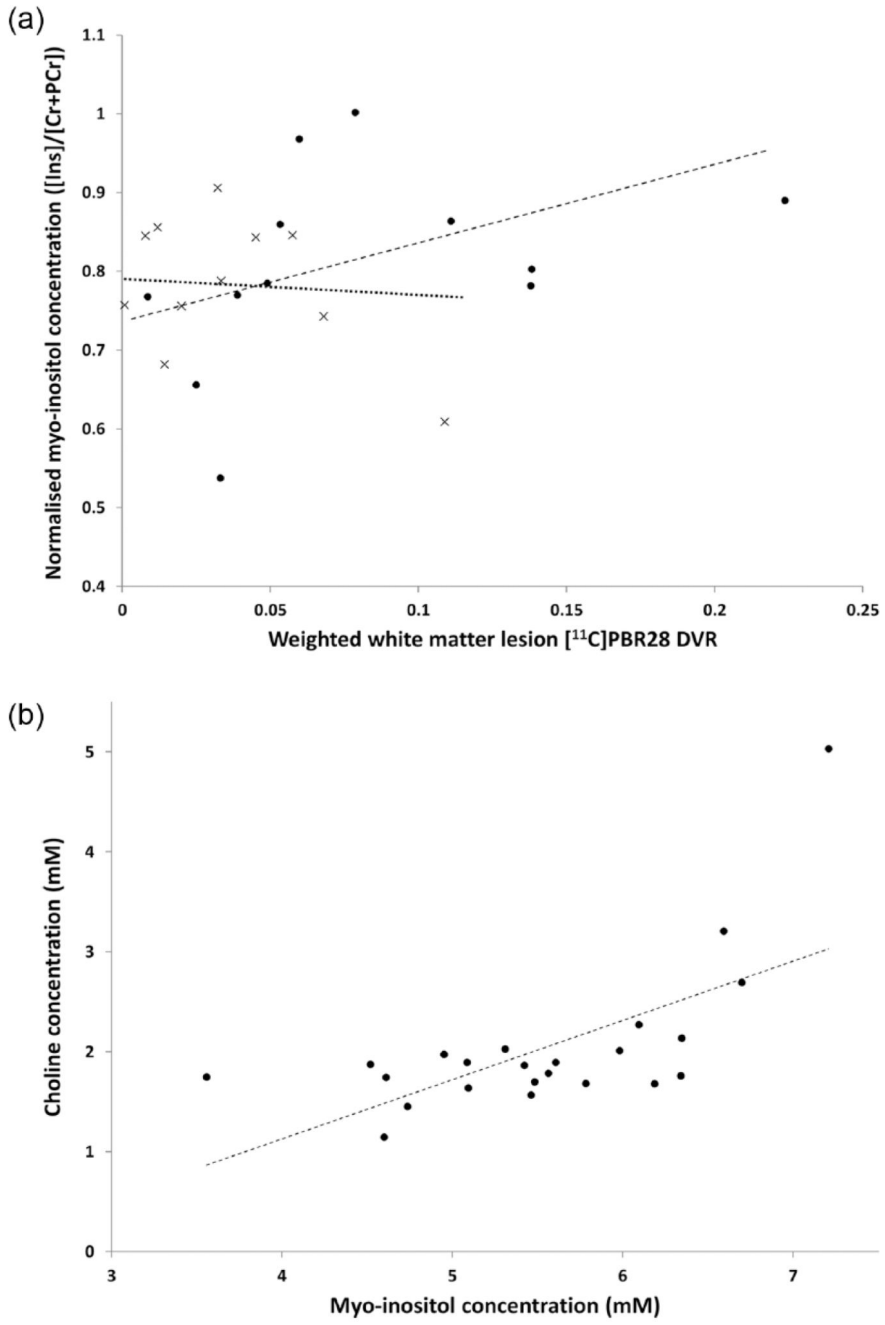

Figure 2.

Relationships of different imaging measures of glial cell activation. (a) Scatter plot of the concentration of myo-inositol ([Ins]) normalised to the total creatine (creatine and phosphocreatine) concentration ([Cr+PCr]) against the [11C]PBR28 distribution volume ratio (DVR) of the T2 FLAIR white matter lesions in the spectroscopy voxel weighted by the white matter lesion tissue fraction. Patients were stratified by group median DVR from the whole spectroscopy voxel (1.26) into those with higher inflammatory load (DVR > 1.26, filled circles) and lower inflammatory load (DVR ⩽ 1.26, crosses). The dashed regression

line describes the *post hoc* correlation found for the higher inflammatory load subgroup (Spearman's $\rho = 0.685$, $p = 0.014$). The dotted regression line represents a best fit for the lower inflammatory load subgroup, which shows no correlation. (b) Correlation of choline to myo-inositol concentration in the spectroscopy voxel ($\rho = 0.547$, $p = 0.007$). The dashed line is the regression line and black dots describe data from different patients ($n = 23$). Concentration is in millimoles (mM).

Europe PMC Funders Author Manuscripts

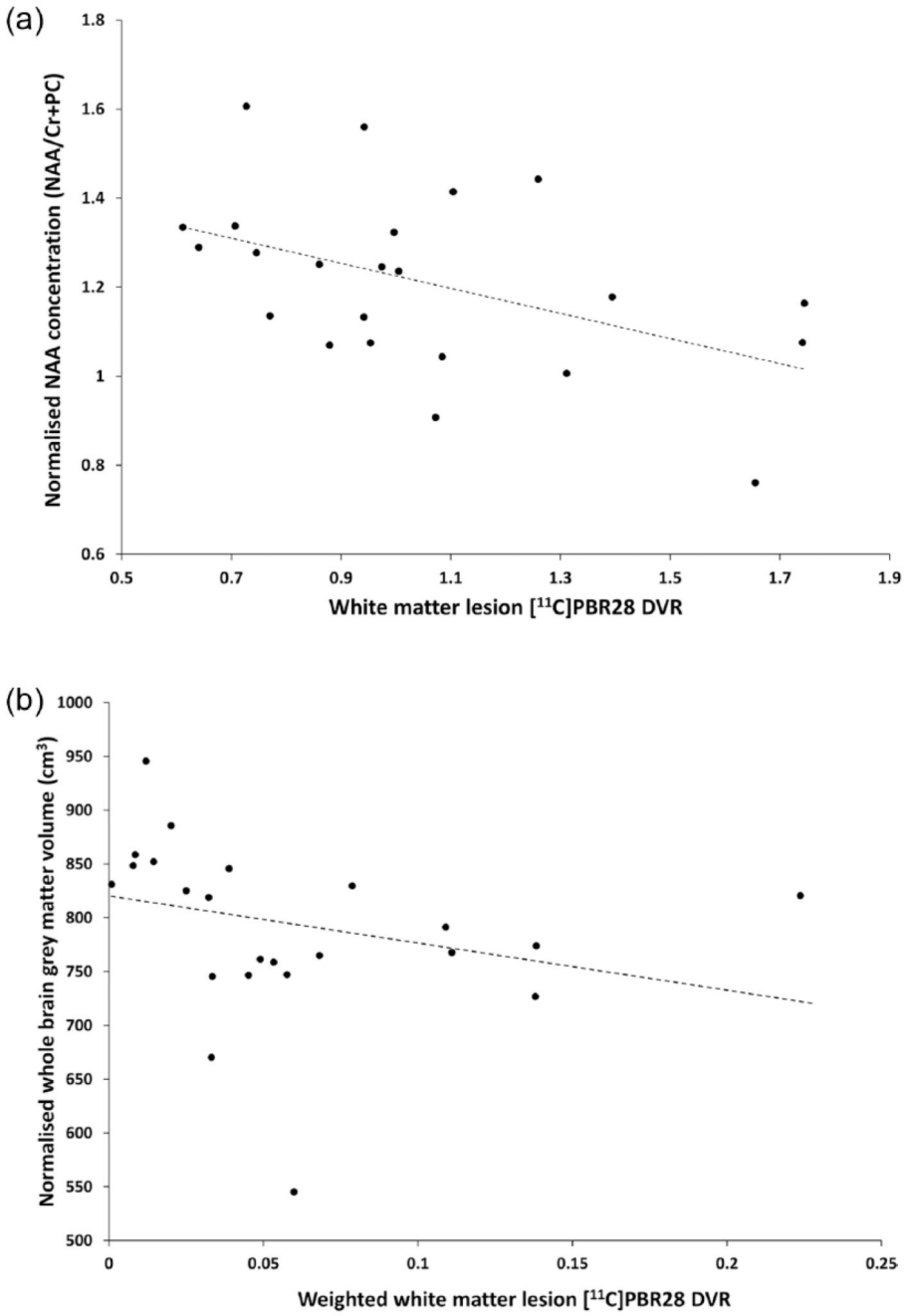

Figure 3.

Correlations of neurodegeneration measures with [11C]PBR28 distribution volume ratio (DVR). (a) The normalised concentration of *N*-acetyl aspartate (NAA) was negatively correlated with the average DVR in T2 FLAIR white matter lesions (Spearman's $\rho = -0.443$, $p = 0.034$). (b) The whole brain normalised grey matter volume was correlated with DVR of white matter lesions within the spectroscopy volume weighted by the white matter

lesion tissue fraction ($\rho = -0.535$, $p = 0.009$). The dashed line is the regression line and black dots describe data from different patients ($n = 23$).

Europe PMC Funders Author Manuscripts

Europe PMC Funders Author Manuscripts

Table 1

Summary of the clinical disability characteristics, grey matter volume and positron-emission tomography (PET) [11C]PBR28 distribution volume ratio for all multiple sclerosis patients.

	Median	Range
EDSS	5.0	1.0 – 7.0
Disease duration (years)	13	1 – 28
MSFC (z-score)	-0.09	-5.99 – 0.69
25FTW (seconds)	7.4	3.3 – 138.4
9HPT (seconds)	23.3	17.7 – 75.2
Whole brain grey matter volume (cm^3)	791	545 – 946
DVR spectroscopy voxel		
Whole voxel	1.26	0.99 – 1.79
White matter lesions	0.97	0.61 – 1.74
NAWM	1.10	0.79 – 1.72
Grey matter	1.44	1.12 – 1.87

EDSS: Expanded Disability Status Scale; MSFC: Multiple Sclerosis Functional Composite; 25FTW: 25 foot timed walk; 9HPT: nine hole peg test; DVR: distribution volume ratio; NAWM: normal-appearing white matter.